

# Networks of Recurrent Events, a Theory of Records, and an Application to Finding Causal Signatures in Seismicity

Jörn Davidsen,<sup>1,\*</sup> Peter Grassberger,<sup>1,2</sup> and Maya Paczuski<sup>1</sup>

<sup>1</sup>*Complexity Science Group, Department of Physics and Astronomy,  
University of Calgary, Calgary, Alberta, Canada T2N 1N4*

<sup>2</sup>*Institute for Biocomplexity and Informatics, University of Calgary, Calgary, Alberta, Canada*  
(Dated: March 31, 2022)

We propose a method to search for signs of causal structure in spatiotemporal data making minimal *a priori* assumptions about the underlying dynamics. To this end, we generalize the elementary concept of recurrence for a point process in time to recurrent events in space and time. An event is defined to be a recurrence of any previous event if it is closer to it in space than all the intervening events. As such, each sequence of recurrences for a given event is a record breaking process. This definition provides a strictly data driven technique to search for structure. Defining events to be nodes, and linking each event to its recurrences, generates a network of recurrent events. Significant deviations in statistical properties of that network compared to networks arising from (acausal) random processes allows one to infer attributes of the causal dynamics that generate observable correlations in the patterns. We derive analytically a number of properties for the network of recurrent events composed by a random process in space and time. We extend the theory of records to treat not only the variable where records happen, but also time as continuous. In this way, we construct a fully symmetric theory of records leading to a number of new results. Those analytic results are compared in detail to the properties of a network synthesized from time series of epicenter locations for earthquakes in Southern California. Significant disparities from the ensemble of acausal networks that can be plausibly attributed to the causal structure of seismicity are: (1) Invariance of network statistics with the time span of the events considered, (2) Appearance of a fundamental length scale for recurrences, independent of the time span of the catalog, which is consistent with observations of the “rupture length”, (3) Hierarchy in the distances and times of subsequent recurrences. As expected, almost all of the statistical properties of a network constructed from a surrogate in which the original magnitudes and locations of earthquake epicenters are randomly “shuffled” are completely consistent with predictions from the acausal null model.

PACS numbers: 02.50.-r, 05.65.+b, 91.30.Dk, 05.45.Tp

## I. INTRODUCTION

Many striking features of physical, biological or social processes can be portrayed as patterns or clusters of localized events. These can be flips of magnetic domains in a ferromagnet leading to Barkhausen noise [1, 2], traffic jams [3], booms and busts of markets and economies [4, 5], forest fires [6], the spread of infections [7] and global pandemics, extinctions of species [4, 8, 9, 10], neural spikes [11], solar flares [12, 13], or earthquakes [14, 15, 16] – to name a few. A generic attribute in all these cases is that one event can trigger or somehow induce another one to occur – or possibly numerous further events. Sometimes, as in the prototype sandpile model [17], an accounting of causes and their effects leads to an interpretation in terms of avalanches – where causal connections between clustered events (“topplings”) are explicitly rationalized by the microscopic state and rules of the dynamical system. More often than not, though, the network of causal connections cannot be resolved from the data at hand and remains ambiguous. Thus, one is often confronted with inferring a plausible

causal structure from clusters of localized events without a detailed or “fundamental” knowledge of the true microscopic dynamics. This remains a stubbornly impenetrable problem despite some progress in special cases (see e.g. Ref. [18] and references therein).

We aim to establish a general procedure of plausible inference based on sequences of data in space and time, or more generally for any temporal sequence of data. The essential idea for the method of analysis discussed here is that of a *recurrence*. Our definition of recurrences is a generalization of “returns” for a point process to higher dimensional data structures that evolve in time. Loosely spoken, a recurrence involves a pair of events which are sufficiently close to each other to suggest a causal connection.

### A. An example of contextual dependence

For illustration consider the two events: (*A*) First, Alice drops a banana, and (*B*) then Bob falls down. If *A* and *B* are sufficiently close in space and time then one can reasonably infer that it is likely that Bob slipped on the banana and fell down (“*A* caused *B*”), but should these events be sufficiently separated then *A* is less likely to have contributed to *B*’s occurrence. For instance, Bob

---

\*Electronic address: davidsen@phas.ucalgary.ca

could have been distracted by the banana, or fell for another reason related to  $A$  without actually slipping directly on the banana – so the two events may still be connected without  $A$  being exclusively the cause of  $B$ . This secondary effect is also less likely if sufficient time has past between the two events. Eventually Alice or another party may pick up the banana or Bob’s fall may have happened so far away that it would be unlikely for him to have slipped on it.

As this example shows, it is not always clear what we should mean by ‘sufficiently close’ to infer a causal connection. One option might be to call a localized event  $B$  a recurrence of an earlier event  $A$ , if its spatial distance is less than some chosen length  $l$  [19]. In addition to introducing a length scale, this choice fails to admit that the plausibility of causal connections typically becomes weaker with time – as the example above makes plain. In addition, the likelihood that the later event ( $B$ ) may be triggered by a third intervening event increases with time as well. These considerations might suggest that  $l$  should shrink with time. On the other hand, the fact that influences usually spread either diffusively or with finite speed could suggest the opposite – that  $l$  increases with time. Spreading of influence is hypothesized, for instance, in theories of “aftershock zone diffusion” (see Ref. [20] and references therein). Other, more complicated scenarios are also conceivable.

This discussion is meant to clarify that without sufficiently accurate *a priori* knowledge of the underlying microscopic dynamics any definition of closeness based on predefined scales is arbitrary and might significantly alter the inferred causal structure. To avoid this problem, or more generally to minimize the influence of the observer, we take the view that, to begin with, a suitable definition of closeness ought to be purely contextual, and depend only on the actual history of events. Taking this as our starting point – that we know the observed history of events but do not know the underlying dynamics – we propose a contextual method to establish recurrences that uses ‘zero knowledge’ of the underlying physical processes. As a result, our definition is generic and can apply to a wide variety of situations. This approach serves as a starting point to analyze data for systems where the underlying dynamics is obscure, mysterious or even misconceived. It comprises a fundamental extension of the concept of recurrences for a point process to recurrent events in space and time that allows the inference of causal relations from available or possible observations.

### B. Contextual relationships represented by a network

In the approach described here, the inferred relationship between each pair of events is based on the closeness of the pair relative to all the other events that have occurred in the data set. An event  $B$  is designated to be a recurrence of a previous one  $A$  if it is closer to  $A$  —

compared to any other event occurring in the time interval between  $A$  and  $B$ . By this construction, each recurrence is a new “record” in the sequence of distances that subsequent events have from  $A$ . In other words, each recurrence is a *record breaking event* [21, 22, 23].

This method of inferring relationships between pairs of events is naturally expressed as a network of connected events where each event is a node in the graph, and each recurrent pair is linked with a time directed edge. Significant deviations in the statistics of the resulting network from that for a random process (which lacks any causal relations between events) highlights relevant parts of the causal dynamical process(es) generating the patterns. In principle, the events themselves do not have to take place in real physical space, but can occur in any space as long as it is equipped with a metric that defines distances. As a starting point, here we only discuss spatiotemporal point processes and take as our test bed a well-characterized, extensive and comparatively accurate catalog [24] of earthquake epicenters for Southern California.

### C. Outline

Section II explains our method for constructing networks of recurrent events and the relation to record breaking statistics. In Section III, the null hypothesis of independent, random events is introduced and a number of analytic results are obtained for it. We extend the mathematical theory of record breaking statistics to the case where both space (or the variable which fluctuates and in which records take place) and time (or the ordering of events) are treated on the same footing. Treating both space and time as continuous symmetrizes the theory – making it more concise. These results allow us to discover statistical features in the actual network of recurrences that are unlikely in acausal random processes and, hence, plausibly due to causal structures in the underlying dynamics.

Section IV describes the application to seismicity. The network analysis reveals new statistical features of seismicity — with robust scaling laws that are invariant over a range of different time scales. This apparent invariance with respect to the time span is diametrically opposed to the behavior for a random process, where all statistical distributions depend explicitly on the time span over which events are recorded. The rupture length and its scaling with magnitude (while being invariant with respect to the time span of the history) emerges from the data analysis without being predefined by the measurement process. It is a generic measure for distance between recurrent events. These results indicate that our method is, indeed, tending to identify causally related events rather than acausal pairs. Further, the relative separations for subsequent recurrences in space (or time) form a hierarchy with unexpected properties. All of these properties disappear when a history constructed

by “shuffling” the original earthquake catalog is analyzed using the same method. In that case, almost all results agree with predictions of the acausal null model. On the basis of these results, we argue that the particular features where we observe strong deviations between the actual history and the acausal null model can be attributed to causal structures in the dynamics of seismicity. We end with a summary and outlook for future works and applications.

## II. SYNTHESIZING THE NETWORK OF RECURRENCES

Consider a series of events  $a_i$ , with  $i = 1 \dots N$ , that are ordered in time such that event  $a_i$  precedes event  $a_j$  if  $i < j$ . The events  $a_i$  are in the following identified with their spatiotemporal position. We assume that a metric is defined in space, and we denote by  $d_{ij}$  the spatial distance between events  $a_i$  and  $a_j$ . Simple examples are spatiotemporal point processes taking place in 3-dimensional Euclidean space or on the surface of a sphere. The only property of the metric relevant to this discussion is that (spatial) distances between all pairs of events can be ordered, e.g. from smallest to largest, and the ordering relation is transitive. The same is of course true for time distances.

The network of recurrent events is defined as follows (see Fig. 1): All events  $a_i$  are represented as nodes and two nodes  $i$  and  $j$  with  $i < j$  are connected by a directed link or edge  $e_{ij}$  if event  $a_j$  is a recurrence of  $a_i$ . This occurs if and only if  $d_{ij} < d_{ik}$  for all  $k$  with  $i < k < j$ . Thus a recurrence is a new record with respect to distance. Note that  $e_{ij}$  and  $e_{ji}$  cannot both exist since the directionality of links is determined by the time ordering. Hence, if  $i < j$  only  $e_{ij}$  can exist. To summarize: the definition of recurrence implies that, for all  $2 < j < n$ , event  $a_j$  is automatically a recurrence of event  $a_{j-1}$  and, thus, all links  $e_{(j-1)j}$  exist. Event  $a_j$  is also a recurrence of any previous event  $a_i$  if it is closer to  $a_i$  than every other event  $a_k$  that occurred in between the two, i.e., for all  $a_k$  with  $i < k < j$ .

As long as only one event occurs at a time, the directed network consists of a single cluster in which each node is linked to at least one other node. Each node  $i$  has an in-degree  $k_i^{in}$ , which is the number of links pointing to it from events in its past, as well as an out-degree  $k_i^{out}$ , which is the number of links emanating from  $i$  – corresponding to the number of records of event  $i$ . The collection of in-nodes  $I_i = \{j \mid e_{ji} \text{ exists}\}$  are hypothesized to reflect the potential cause(s) of event  $a_i$  while the set of out-nodes  $O_i = \{j \mid e_{ij} \text{ exists}\}$  are hypothesized to contain the effect(s) of  $a_i$ . Although it is natural to contemplate associating a weight factor to each link, this requires further assumptions. Here we do not deal with this issue and consider all links to have the same weight. This is in our view a “zeroth order” assignment of causes and their effects based purely on the history of events and

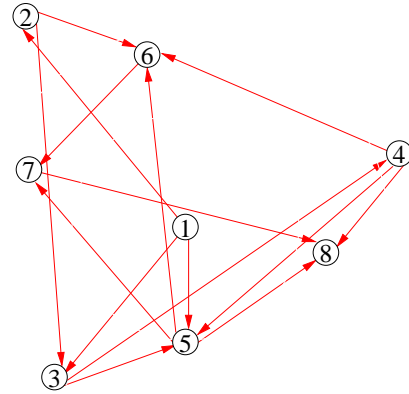


FIG. 1: Eight events in 2D space labelled according to their order of occurrence in time. The network of recurrences is indicated by arrows as described in the text.

their relationships to each other in space and time. Note that a single event can have many causes corresponding to all of its incoming links, so the network aspect of causal relations is not lost in this limit. Weighted networks of seismic events were constructed using a different methodology in Refs. [16, 25, 26].

While this network construction, based on record breaking events, is directly applicable to fixed collections of events, it can also be applied when the number of events  $N$  increases over time. The result of adding a new event  $a_{N+1}$  is to increase the number of links by at least one, namely  $e_{N(N+1)}$ , without altering any pre-existing links. Hence, the property of being a recurrence is *preserved* in all cases under addition of new nodes in time. Also the collections of in-nodes for all pre-existing nodes remains unchanged. Yet, the out-degree of any node  $i$  with  $i < N + 1$  can increase by one, namely if  $a_{N+1}$  is a recurrence of  $a_i$ . So the networks are, in this sense, dynamically stable growing networks [27, 28].

Some tools and measures already exist to quantify statistical topological features of networks, and to reveal the organization of the dynamical process(es) giving rise to the events in terms of network statistics [27, 28]. The dependence of the network statistics can be examined by varying the time span of the history synthesized into a network, space window over which the history is observed, and/or selection criteria for what is defined as an event (in the seismic application discussed later, this could e.g. be the range of earthquake magnitudes). Our approach opens up a new view of dynamical organization of spatiotemporal activity in terms of the (static) topology of complex networks – as was also discussed in [16, 25, 26, 29, 30]. We also believe it possible that new developments in network theory may turn out to be even more powerful in analyzing dynamical systems. For

the work described here, standard methods of network analysis are already sufficient to plausibly infer certain causal relations in seismic behavior solely from the catalog of earthquake magnitudes, epicenter locations and times.

### III. THE ACAUSAL NULL MODEL AND A THEORY OF RECORDS

#### A. General remarks

In order to be able to associate causal characteristics of the dynamics to the network of recurrences, we mathematically establish statistical properties of a null model, where the events in space and time are random, uncorrelated and causally unrelated. Then any statistically significant deviation of the observed network from this null hypothesis can be attributed to correlations among events and to causal structure in the underlying dynamics giving rise to the observed history. The conclusions about the relation to causality are robust as long as the relevant properties of any acausal null model are well represented by those we study.

In the following we shall discuss several variants of the null model. In all of them, both space and time are continuous. To the best of our knowledge, the theory of records has up to now been developed only for discrete time and continuous space [21, 22, 23]. As we shall see, when both variables are continuous the core of the theory becomes symmetric under exchange of space and time, allowing for a more concise formulation. This symmetry is obviously lost when making one of the variables discrete.

Let us denote by  $\rho(\mathbf{x}_1, t_1; \dots \mathbf{x}_n, t_n)$  the joint probability density for having events at locations  $(\mathbf{x}_i, t_i)$ ,  $i = 1, \dots, n$ . Our basic assumptions are that:

(a) Events are independent and identically distributed (iid),

$$\rho_n(\mathbf{x}_1, t_1; \dots \mathbf{x}_n, t_n) = \prod_{i=1}^n \rho_1(\mathbf{x}_i, t_i). \quad (1)$$

(b) The single-event distributions factorize,

$$\rho_1(\mathbf{x}, t) = \rho_x(\mathbf{x})\rho_t(t). \quad (2)$$

In particular, when  $\rho_t(t) = \text{const}$ , Eq. (2) means that we have a stationary system. Note that  $\int d\mathbf{x} dt \rho_1(\mathbf{x}, t) = N$ , the total average number of events in the history, as long as this number is finite.

Instead of event distributions themselves, we shall in the following use the distributions of space-time distances relative to some reference event or “Event-0” at  $(\mathbf{x}_0, t_0)$ ,

$$\begin{aligned} \mu_n(l_1, t_1; \dots l_n, t_n) &= \prod_{i=1}^n \int d\mathbf{y}_i \delta(|\mathbf{x}_0 - \mathbf{y}_i| - l_i) \times \\ &\rho_n(\mathbf{x}_0, t_0; \mathbf{y}_1, t_0 + t_1; \dots \mathbf{y}_n, t_0 + t_n). \end{aligned} \quad (3)$$

It is easily seen that these joint distributions also factorize under the above assumptions as,

$$\mu_n(l_1, t_1; \dots l_n, t_n) = \prod_{i=1}^n \mu_1(l_i, t_i) \quad (4)$$

with

$$\mu_1(l, t) = \mu_l(l)\mu_t(t). \quad (5)$$

The functions  $\mu_l(l)$  and  $\mu_t(t)$  might in general depend on the reference point,  $\mathbf{x}_0$ . We will not indicate this dependence explicitly, unless it is relevant for the calculation.

First, we consider the special case  $\mu_l(l) = \mu_t(t) = 1$ , which holds if the system is stationary, 1-dimensional, homogeneous, and has the suitable space-time density of events. The next step is when either one of these functions or both are equal to one up to finite cut-offs and zero beyond, i.e.  $\mu_l(l) = \Theta(\lambda - l)$  and/or  $\mu_t(t) = \Theta(\sigma - t)$ . Physically,  $\lambda$  is not only the maximal possible distance between two events (due to finiteness of space), but it is also the rate at which events occur per unit time, if  $\mu_t(t) = 1$ . Similarly, a finite value of  $\sigma$  indicates not only that events are observed in a finite time window, but also that the average number of events per unit distance is finite.

#### B. Canonical coordinates

Fortunately, it is sufficient to discuss these simple cases, because for any non-singular densities  $\mu_l(l)$  and  $\mu_t(t)$  the problem can be reduced to one of them by a change of coordinates. Consider the two transformations

$$\xi = \int_0^l dl' \mu_l(l'), \quad \tau = \int_0^t dt' \mu_t(t'). \quad (6)$$

Clearly,  $\xi$  is a positive and monotonically increasing function of  $l$ , while  $\tau$  is a positive and monotonically increasing function of  $t$ . Due to conservation of probability, both have unit density

$$\mu_\xi(\xi) = \Theta(\lambda - \xi), \quad \mu_\tau(\tau) = \Theta(\sigma - \tau), \quad (7)$$

where we have denoted by  $\lambda$  and  $\sigma$  the integrals over  $\mu_l$  and  $\mu_t$ , respectively,

$$\lambda = \int_0^\infty dl' \mu_l(l'), \quad \sigma = \int_0^\infty dt' \mu_t(t'). \quad (8)$$

Thus, the distributions of events in  $\xi$  and  $\tau$  are cut-off sharply at  $\lambda$  and  $\sigma$ , respectively. Note that  $\lambda$  and  $\sigma$  can be infinite.

Thus, for general space and time distributions, we can first do all calculations in the “canonical coordinates”  $\xi$  and  $\tau$ , and then translate the results, using inverse transformations of Eq. (6), back to the original coordinates  $l, t$ . Examples are given below. In the following we always assume that  $\xi$  and  $\tau$  are defined by Eq. (6) and, thus, Eq. (7) holds for all positive  $\xi$  and  $\tau$ .

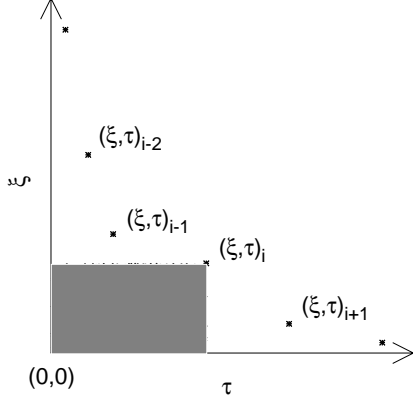


FIG. 2: A typical chain of recurrences in canonical coordinates. The reference event or Event-0 for all these recurrences is at the origin  $\tau = \xi = 0$ . The event at  $(\xi_i, \tau_i)$  is a recurrence of the event at  $(0,0)$  if and only if no event is in the shaded region.

In canonical coordinates, a typical sequence of recurrences is drawn schematically in Fig. 2. For all recurrences  $i$ ,  $\xi_{i+1} < \xi_i$  and  $\tau_{i+1} > \tau_i$ . This is symmetric under the exchange  $\xi \leftrightarrow \tau$ ,  $\lambda \leftrightarrow \sigma$ , and  $i \leftrightarrow -i$ . The probability that a given event  $(\xi, \tau)$  is a recurrence of Event-0 at  $(0,0)$  is equal to the chance that no event occurred in the rectangular region  $[0, \tau] \times [0, \xi]$ , which is equal to  $\exp(-\xi\tau)$  due to the unit space-time density of events in the  $(\xi, \tau)$ -plane. Hence, the joint probability density function (PDF) of *recurrences* is given by the same exponential,

$$p(\xi, \tau) = e^{-\xi\tau}, \quad (9)$$

except for the possible cut-offs at  $\lambda$  and/or  $\sigma$ , beyond which the density of recurrences is zero;  $p(\xi > \lambda, \tau) = p(\xi, \tau > \sigma) = 0$ .

### C. Infinite space and time domains

For a detailed discussion of the spatial and temporal distributions of recurrences we deal separately with the cases of finite and infinite  $\lambda$  and/or  $\sigma$ . We first consider the case where neither  $\mu_l(l)$  nor  $\mu_t(t)$  is normalizable, i.e.  $\lambda = \sigma = \infty$ . This, for example, describes the case of stationary and homogeneous systems in infinite  $D$ -dimensional Euclidean space, where  $\mu_t(t) = \text{const}$  and  $\mu_l(l) \propto l^{D-1}$ . But it holds also approximately for fractal distributions in space (if we neglect effects of lacunarity [31]), with  $D$  being the fractal dimension. Notice that  $\int_0^\infty dl l^{D-1} = \infty$  for all values of  $D$ .

The spatial and temporal density distributions of recurrences in canonical coordinates are obtained by integrating Eq. (9) to obtain the marginals,

$$p_\xi(\xi) = \int_0^\infty d\tau p(\xi, \tau) = 1/\xi, \quad (10)$$

$$p_\tau(\tau) = \int_0^\infty d\xi p(\xi, \tau) = 1/\tau. \quad (11)$$

Assuming that the system is translationally invariant in time and fractal in space, i.e.  $\mu_t(t) = b = \text{const}$  and  $\mu_l(l) = aDl^{D-1}$ , we obtain for the densities in the original coordinates

$$p_l(l) = \mu_l(l)p_\xi(\xi(l)) = \frac{aDl^{D-1}}{al^D} = D/l, \quad (12)$$

$$p_t(t) = \mu_t(t)p_\tau(\tau(t)) = b[bt]^{-1} = 1/t. \quad (13)$$

Thus the recurrence density in time is independent of the event rate (per unit space-time region). Similarly, for an event distribution with given (fractal or Euclidean) non-trivial dimension, the recurrence density depends on the dimension but not on the parameter  $a$ . Also, notice that  $p_t(t)$  is completely independent of the spatial event distribution  $\mu_l(l)$ , and  $p_l(l)$  is independent of  $\mu_t(t)$ .

For homogeneous and mono-fractal stationary spatial distributions both  $p_t$  and  $p_l$  are independent of the reference point defining the recurrences. This is no longer true for multifractals, where  $p_l(l)$  depends on the local (point-wise) dimension at the event which defines the recurrences.

The analog of Eq. (13) for discrete time is a classic result in the theory of records [21, 22, 23]. In contrast, Eq. (12) was first reported in [29], as far as we know.

### D. Finite space and infinite time — and vice versa

Let us assume that  $\mu_t(t)$  is not normalizable but  $\mu_l(l)$  is,

$$\lambda < \infty, \quad \sigma = \infty. \quad (14)$$

Now, of course,  $p_\xi(\xi) = 0$  for  $\xi > \lambda$ . For  $\xi < \lambda$ , on the other hand,  $p_\xi(\xi)$  is still given by integrating  $\exp(-\xi\tau)$  over all positive values of  $\tau$  as in Eq. (10), i.e.

$$p_\xi(\xi) = \frac{1}{\xi} \Theta(\lambda - \xi). \quad (15)$$

In terms of the original coordinates, one finds

$$p_l(l) = \mu_l(l)p_\xi(\xi(l)) = \frac{\mu_l(l)}{\int_0^l dl' \mu_l(l')}. \quad (16)$$

In contrast,  $p_\tau(\tau)$  is obtained by integrating Eq. (9) over the finite domain  $0 < \xi < \lambda$ , which gives

$$p_\tau(\tau) = \frac{1}{\tau} (1 - e^{-\lambda\tau}). \quad (17)$$

In the stationary case, when  $t$  is just proportional to  $\tau$ , the density of recurrences in  $t$  is given by the same formula with  $\lambda$  replaced by the rate of events per unit  $t$ . The additional term compared with Eqs. (11) and (13) reflects the probability that no recurrence occurs up to time  $\tau$  and  $t$ , respectively.

In the opposite case ( $\lambda < \infty$ ,  $\sigma = \infty$ ) of finite event rate per unit distance and infinite rate per unit time (corresponding typically to infinite space and finite time, with finite space time density of events), the situation is completely symmetric. In that case  $p_\tau(\tau)$  is cut-off sharply at a finite value, while  $p_\xi(\xi)$  is cut-off with an exponential correction term as in Eq. (17).

### E. Finite space and finite time

Now both  $p_\xi(\xi)$  and  $p_\tau(\tau)$  are obtained by integrating Eq. (9) over finite domains,

$$p_\xi(\xi) = \frac{1}{\xi} \Theta(\lambda - \xi)(1 - e^{-\sigma\xi}), \quad (18)$$

$$p_\tau(\tau) = \frac{1}{\tau} \Theta(\sigma - \tau)(1 - e^{-\lambda\tau}). \quad (19)$$

Thus,  $p_\xi(\xi)$  asymptotically approaches the constant  $\sigma$  in the limit  $\xi \rightarrow 0$  while for intermediate arguments we recover the  $1/\xi$  decay for infinite space and time domains given in Eq. (10). For large arguments, the density sharply drops to zero at  $\xi = \lambda$ .  $p_\tau(\tau)$  asymptotically approaches the constant  $\lambda$  in the limit  $\tau \rightarrow 0$  while for intermediate arguments we recover the  $1/\tau$  decay for infinite space and time domains given in Eq. (11). For large arguments, the density sharply drops to zero at  $\tau = \sigma$ . The respective transition points  $\xi^*$  and  $\tau^*$  between the constant behavior for small arguments and the decaying behavior for intermediate arguments can be defined in the standard way by requiring that the argument of the exponential equals  $-1$ , i.e.,

$$\sigma\xi^* \equiv 1, \quad (20)$$

$$\lambda\tau^* \equiv 1. \quad (21)$$

Specific realizations of such a process include stationary systems observed over a finite time window, where events occur only in a finite region of space — or are only recorded when they fall into that region. One example is  $\mu_t(t) = b\Theta(T - t)$  and  $\mu_l(l) = aDl^{D-1}\Theta(R - l)$  with positive constants  $T$  and  $R$ . In this case, Eq. (18) translates into

$$p_l(l) = \begin{cases} abTDl^{D-1} & \text{for } l \ll l^*(T), l < R, \\ D/l & \text{for } l \gg l^*(T), l < R, \\ 0 & \text{for } l > R, \end{cases} \quad (22)$$

and Eq. (19) translates into

$$p_t(t) = \begin{cases} abR^D & \text{for } t \ll t^*(L), t < T, \\ 1/t & \text{for } t \gg t^*(L), t < T, \\ 0 & \text{for } t > T, \end{cases} \quad (23)$$

with

$$l^*(T) \equiv (abT)^{-1/D}, \quad (24)$$

and

$$t^*(L) \equiv [abR^D]^{-1}. \quad (25)$$

Finally, let  $\langle N \rangle = abTR^D$  be the average total number of observed events. Then the expressions for the transition points are particularly simple

$$l^*(N) = L/\langle N \rangle^{1/D}, \quad (26)$$

$$t^*(N) = T/\langle N \rangle. \quad (27)$$

In this simple example and in the situations discussed in subsection III D, we have assumed that translational invariance holds. However, this is generally not true. Specific realizations of such processes include stationary systems observed over a *fixed* finite time window, where events occur only in a *fixed* finite region of space — or are only recorded when they fall into that region. Due to the lack of translational invariance, the distributions of distances (spatial and temporal) between events depend on the defining event. We discuss the consequences of broken translational invariance now.

For concreteness and simplicity, let us assume a stationary system where events occur uniformly on an interval  $0 < x < L$  with periodic boundary conditions, with space-time density  $\alpha$ . They are recorded only in the time window  $0 < t < T$ . In general, the distributions of distances between events in a bounded space-time region depend on the reference point  $(x_0, t_0)$ , but in the present case this simplifies due to the periodic boundary condition: The recurrence distributions depend on  $t_0$ , but not on  $x_0$ . More precisely,

$$\mu_l(l; x_0, t_0) = 2\alpha\Theta(L/2 - l), \quad (28)$$

$$\mu_t(t; x_0, t_0) = \Theta(T - t_0 - t),$$

for positive arguments  $t$  and  $l$ , respectively. Note that the asymmetrical attribution of the factor  $\alpha$  to  $\mu_l$  is arbitrary.

This *ansatz* gives  $\sigma = (T - t_0)$  and  $\lambda = \alpha L$ . The relations between original and canonical coordinates are

$$\xi(l) = \begin{cases} 2\alpha l & 0 < l < L/2 \\ \alpha L & l > L/2, \end{cases} \quad (29)$$

$$\tau(t) = \begin{cases} t & 0 < t < T - t_0 \\ T - t_0 & t > T - t_0. \end{cases} \quad (30)$$

The recurrence PDFs are obtained by inserting this into Eqs. (18,19) and transforming back to the original coordinates. The *average* distributions of distances between recurrences and reference points are obtained by averaging over  $t_0$ . The final results are

$$\langle p_l(l) \rangle_{t_0} = \frac{1}{l} \left[ 1 - \frac{1 - e^{-2\alpha l T}}{2\alpha l T} \right] \Theta(L/2 - l), \quad (31)$$

$$\langle p_t(t) \rangle_{t_0} = \frac{1}{t} (1 - e^{-\alpha L t}) (1 - \frac{t}{T}) \Theta(T - t), \quad (32)$$

These detailed results are included in order to demonstrate that exact calculations are possible in the most simple case. But in more realistic cases no exact results can be expected. As a general rule, the simple power

laws of Eqs. (12,13) will hold for intermediate values of  $l$  and  $t$ , but corrections will be necessary both for large and for small  $l$  and  $t$  – as follows from Eqs. (18,19). The corrections render the distributions finite at small values of the arguments, and they cut them off at large ones.

The cut-offs at large  $l$  and  $t$  occur just at the sizes of the system. Their detailed shapes depend, as suggested by comparing Eqs. (31,32) with Eqs. (22,23), on the specific properties of the system at large scales. The behavior at small distances is more general.

To see this, let us consider Eq. (32) in more detail. There the deviation from the infinite system limit happens when  $\alpha t L \approx 1$ , i.e. at a time

$$t \approx t^*(L) \equiv (\alpha L)^{-1} \quad , \quad (33)$$

which exactly coincides with Eq. (25) for the translational invariant case. Since  $\alpha$  is the density of events in space-time,  $t^*$  is the average time delay between successive events. Obviously, *recurrences* cannot follow each other faster than *events*. Similarly in Eq. (31), the deviation from the infinite system limit happens when  $2\alpha l T \approx 1$ , which coincides with the expression for  $l^*(T)$  in the translational invariant case given by Eq. (24).

Not only is the scaling of  $l^*$  and  $t^*$  identical to the translationally invariant case but also the qualitative behaviors of  $\langle p_l(l) \rangle_{t_0}$  and of  $\langle p_t(t) \rangle_{t_0}$  for  $l \ll l^*$  and  $t \ll t^*$ , respectively, are identical. This strongly suggests that the results given in Eqs. (22,23,24,25) capture the essential behavior for scales smaller than the large scale cut-off – even when translational invariance is explicitly broken.

## F. Correlations between recurrences and properties of recurrences with fixed rank

Let  $p(l, t; l', t')$  be the PDF that two events at space-time positions  $(l, t)$  and  $(l', t')$  are both records – not necessarily subsequent ones. Referring to Fig. 2, and using Bayes' theorem in canonical coordinates, we are interested in the probability that no other event occurs in either of the two rectangles associated to the events, which is determined by the union of the two rectangular areas. Hence if  $\tau > \tau'$  and  $\xi < \xi'$ , then

$$p(\xi, \tau; \xi', \tau') = e^{-\xi\tau - (\xi' - \xi)\tau'} \Theta(\sigma - \tau) \Theta(\lambda - \xi') \quad . \quad (34)$$

This directly determines  $p(l, t; l', t')$ .

Integrating over  $\xi$  and  $\xi'$  gives the joint PDF for having recurrences at times  $\tau$  and  $\tau'$ ,

$$\begin{aligned} p(\tau, \tau') &= \int_0^\lambda d\xi' \int_0^{\xi'} d\xi e^{-\xi\tau - (\xi' - \xi)\tau'} \Theta(\sigma - \tau) \\ &= \frac{1}{\tau\tau'} \left[ 1 - \frac{\tau e^{-\lambda\tau'} - \tau' e^{-\lambda\tau}}{\tau - \tau'} \right] \Theta(\sigma - \tau) \end{aligned} \quad (35)$$

For  $\lambda = \infty$ , this gives  $p(\tau, \tau') = (\tau\tau')^{-1}$ , for  $\tau' < \tau < \sigma$  so the two recurrences are uncorrelated. For finite  $\lambda$ ,

records are correlated; i.e.  $p(\tau, \tau') \neq p_\tau(\tau)p_{\tau'}(\tau')$ . For a stationary process, these results hold in the original coordinate  $t$  as well.

Alternatively, let  $q(l, t; l', t')$  be the probability that two events at  $(l, t)$  and  $(l', t')$  are *successive* records. Assuming again that  $\tau > \tau'$  and  $\xi < \xi'$ , we now demand that both are records, as above, and also that no other *event* happens in the rectangle  $[\xi', \xi] \times [\tau', \tau]$ , or

$$q(\xi, \tau; \xi', \tau') = e^{-\xi'\tau} \Theta(\lambda - \xi') \Theta(\sigma - \tau) \quad . \quad (36)$$

Integrating over  $\xi$  and  $\xi'$  gives the joint PDF for having successive records at times  $\tau$  and  $\tau'$  to be

$$\begin{aligned} q(\tau, \tau') &= \int_0^\lambda d\xi' \int_0^{\xi'} d\xi e^{-\xi'\tau} \Theta(\sigma - \tau) \\ &= \frac{1}{\tau^2} [1 - (1 + \lambda\tau)e^{-\lambda\tau}] \quad \text{for } \tau' < \tau < \sigma \quad . \end{aligned} \quad (37)$$

Hence, times to successive recurrences are always correlated. When  $\lambda = \infty$ , the joint PDF is  $q(\tau, \tau') = 1/\tau^2$  for  $\tau' < \tau < \sigma$ .

For the PDF of the ratio of the times of successive records  $x = \tau'/\tau > 0$ , it directly follows for finite  $\lambda$  that

$$\begin{aligned} q_\tau(x) &= \int_0^{\sigma x} d\tau' q(\tau(x), \tau') \left| \frac{d\tau}{dx} \right| \\ &= \Theta(1 - x) \sum_{i=1}^{\infty} \frac{(i-1)(-\lambda\sigma)^i}{i \cdot i!} \quad , \end{aligned} \quad (38)$$

which is constant in the interval  $[0; 1]$ . This is also the result in the original coordinates, if the system is stationary – in which case  $t \propto \tau$  and  $x = t'/t$ .

We now discuss spatial distance distributions of recurrences with fixed rank  $i$ , and first consider a finite stationary system infinitely extended in time ( $\sigma = \infty$ ). Let  $p_\xi^{(i)}(\xi)$  be the spatial distance PDF for the  $i$ -th recurrence following Event-0. For any  $i \geq 2$ , the recursion relation

$$p_\xi^{(i)}(\xi) = \int_\xi^\lambda d\xi' q(\xi|\xi') p_\xi^{(i-1)}(\xi') \quad , \quad (39)$$

exists. The quantity  $q(\xi|\xi')$  is the conditional PDF, given that the previous recurrence happened at distance  $\xi'$ , for the distance of the next recurrence. One easily shows that

$$q(\xi|\xi') = \frac{1}{\xi'} \Theta(\xi' - \xi) \quad (40)$$

independently of  $i$ , so that

$$p_\xi^{(i)}(\xi) = \int_\xi^\lambda \frac{d\xi'}{\xi'} p_\xi^{(i-1)}(\xi') \quad . \quad (41)$$

The solution for finite  $\lambda$  is

$$p_\xi^{(i)}(\xi) = \frac{\Theta(\lambda - \xi)}{(i-1)!} \left( \ln \frac{\lambda}{\xi} \right)^{i-1} \quad . \quad (42)$$

If the event density in original coordinates was  $\mu(l) = aDl^{D-1}\Theta(R-l)/R^D$ , i.e., confined to a disc with radius  $R$ , then the last equation translates into

$$p_l^{(i)}(l) = a\Theta(R-l) \frac{D^i l^{D-1}}{(i-1)!R^D} (\ln R/l)^{i-1}, \quad (43)$$

while Eq. (40) gives for the PDF of the ratio  $x = l/l' > 0$

$$q_l(x) = Dx^{D-1}\Theta(1-x). \quad (44)$$

These last results have to be modified when  $\sigma < \infty$ , i.e. when there is a finite observation window in time. In that case we are not guaranteed that at least  $i$  recurrences exist, and thus  $p_l^{(i)}(l)$  has to be replaced by the conditional PDF, conditioned on the existence of  $\geq i$  recurrences. That requires a more extensive development than we take up here.

### G. Distribution of the number of recurrences – or the degree distributions

The out-degree distribution  $P^{out}(k, N)$  is the probability that a randomly chosen event out of a sequence of  $N$  events has  $k$  records. This probability can be deduced using previous results from the theory of records [21, 22, 23, 32, 33]. We assume that the system is stationary, with a finite rate of events per unit time. We denote the event defining recurrences as Event-0. We use the fact that recurrences are records in the sense that each recurrence is an event that is closer to Event-0 than all previous events that happened after Event-0. Consider a series of  $i$  events following Event-0. The probability that event  $j$  is a record is  $1/j$  and the probability that it is not is  $(j-1)/j$ . Hence the probability that there is precisely one record in a series of  $i$  events following Event-0 is  $P_i(1) = \prod_{j=2}^i (j-1)/j = 1/i$ . Notice that the first event after Event-0 is always a record. The probability that there are precisely two records in the series of  $i$  events is

$$P_i(2) = \left( \prod_{j=2}^i \frac{j-1}{j} \right) \sum_{l_1=2}^i \left( \frac{l_1}{l_1-1} \times \frac{1}{l_1} \right) = \frac{1}{i} \sum_{l_1=2}^i \frac{1}{l_1-1}. \quad (45)$$

Continuing with standard methods it is possible to show that the probability of finding precisely  $k$  records in a series of  $i$  events,  $P_i(k)$ , is given by

$$\begin{aligned} P_i(k) &= \frac{1}{i} \sum_{1 < l_1 < \dots < l_{k-1} \leq i} \frac{1}{(l_1-1) \dots (l_{k-1}-1)} \\ &= \frac{|S_i^k|}{i!} \\ &\approx \frac{(\ln i)^{k-1}}{i(k-1)!}, \end{aligned} \quad (46)$$

where the symbol  $S$  indicates Stirling's number of the first kind and the last expression holds for  $i \gg k \gg 1$ .

Considering that each event except the last one in the sequence of  $N$  events initiates its own sequence of records, and hence is an Event-0, gives

$$P^{out}(k, N) \approx \frac{1}{N} \sum_{i=1}^{N-1} \frac{(\ln i)^{k-1}}{i(k-1)!} \approx \frac{(\ln(N))^k}{N k!}, \quad (47)$$

where the last step involves approximating the sum as an integral, which is valid for large  $N$ . Therefore, the out-degree distribution for a random process of  $N \gg 1$  events is a Poisson distribution with mean degree  $\langle k \rangle \approx \ln N$  [33].

Furthermore, the probability to have out-degree one,  $P^{out}(1, N)$ , can be computed exactly [21, 33]: For those nodes the closest event in space is also the closest in time. For event  $i$ , this happens with probability  $1/(N-i)$ . Thus,

$$P^{out}(1, N) = N^{-1} \sum_{i=1}^{N-1} \frac{1}{N-i} \approx \frac{\ln(N) + e_M}{N}, \quad (48)$$

where we have approximated the harmonic series by the corresponding integral and  $e_M \approx 0.58$  is the Euler-Mascheroni constant. Note that Eq. (48) is exact in the limit  $N \rightarrow \infty$ .

For the in-degree distribution,  $P^{in}(k, N)$ , similar considerations apply: Event  $i$  is a recurrence of event  $j$  ( $0 \leq j < i$ ) with probability  $1/(i-j)$ , which is independent of  $N$ . This allows to compute the in-degree distribution  $P_i^{in}(k)$  of event  $i$ :

$$\begin{aligned} P_i^{in}(k) &= \frac{1}{i} \sum_{l_1=0}^{i-k} \sum_{l_2=l_1+1}^{i-k+1} \dots \sum_{l_{k-1}=l_{k-2}+1}^{i-1} \frac{1}{l_1 l_2 \dots l_{k-1}} \\ &= \frac{|S_i^k|}{i!} \\ &\approx \frac{(\ln(i))^{k-1}}{i(k-1)!}, \end{aligned} \quad (49)$$

for  $0 < k \leq i-1$  and zero otherwise. Hence

$$P^{in}(k, N) = \frac{1}{N} \sum_{i=1}^{N-1} P_i^{in}(k) \approx \frac{(\ln(N))^k}{N k!}. \quad (50)$$

As expected for a fully random process,  $P^{in}(k, N)$  is identical to  $P^{out}(k, N)$  and well-approximated by a Poisson distribution with mean degree  $\langle k \rangle \approx \ln N$  for  $N \gg 1$ .

### H. Degree correlations

Due to the acausal nature of the null model, the joint probability  $P_i(k^{in}, k^{out})$  that event  $i$  has in-degree  $k^{in}$  and out-degree  $k^{out}$  factors for all nodes  $i$ . As a result

$$\begin{aligned} P_i(k^{in}, k^{out}) &= P_{N-i}(k^{out}) P_i^{in}(k^{in}) \\ &\approx \frac{(\ln(N-i))^{k^{out}-1}}{(N-i)(k^{out}-1)!} \frac{(\ln(i))^{k^{in}-1}}{i(k^{in}-1)!} \end{aligned} \quad (51)$$



This allows us to compute the mean out-degree of all events with a given in-degree in a sequence of  $N$  events

$$\langle k^{out} \rangle(k^{in}, N) = \sum_{k^{out}=0}^{N-1} k^{out} \frac{1}{N} \sum_{i=1}^{N-1} P_i(k^{in}, k^{out}) / P^{in}(k^{in}, N) \approx 1 + \frac{1}{(\ln(N-1))^{k^{in}}} \int_1^{N-1} \frac{(\ln(i))^{k^{in}}}{N-1-i} di \quad (52)$$

The out-degree  $\langle k^{out} \rangle$  weakly depends on  $k^{in}$  due to the fact that the rank of each event implicitly couples its in- and out-degree in a finite sequence of events. For instance, if the rank of an event is small (large) compared to  $N$ , the in-degree is more likely to be small, but the out-degree is more likely to be large. Consequently,  $\langle k^{out} \rangle(k^{in}, N)$  decreases with  $k^{in}$  for fixed  $N$ . For similar reasons, weak correlations also appear between the in-/out-degree of a node and the in-/out-degree of its recurrences. For example, a large (small) in-degree for a node implies on average a small (large) out-degree for its recurrences. Similarly, the out-degree (in-degree) of recurrences increases on average with the out-degree (in-degree) of their Event-0.

#### IV. APPLICATION TO SEISMIC PATTERNS

Seismicity is a prime example where localized events in space and time can be accurately and, with certain caveats, exhaustively recorded. It is also a phenomenon where the causal features of the dynamics responsible for the patterns are subject to ongoing debate and uncertainty. Seismic data involving many earthquakes occurring over large regions of space and time exhibit a number of regularities. These include clustering, fault traces and epicenter locations with fractal statistics, as well as scaling laws like the Omori and Gutenberg-Richter (GR) laws (see e.g. Refs. [14, 15, 34] for a review). Given that the associated earthquake patterns in space and time are readily observable, approaches based on the concept of spatiotemporal point processes have been amply demonstrated to be feasible [16, 35, 36, 37, 38, 39]. In that case, the description of seismicity is reduced to recording the size or magnitude of each earthquake, its epicenter and its time of occurrence.

To test the suitability of our method to characterize seismicity in a way that makes it possible to infer relevant causal features of its dynamics and to extend our earlier analysis [29], we study a “relocated” earthquake catalog from Southern California [24]. The catalog has improved relative location accuracy within clusters of similar events, the estimated horizontal standard errors being typically less than 50 to 100m and the estimated vertical standard errors being typically less than 100 to 200m [40, 41]. Due to the higher relative and absolute location errors for the depth of an earthquake,

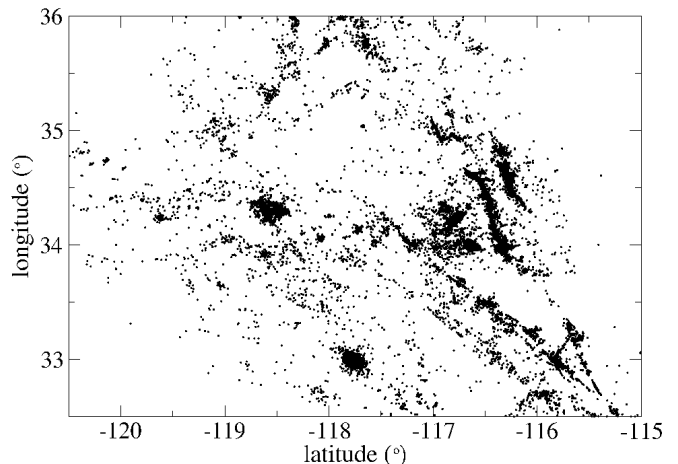


FIG. 3: (Color online) Spatial pattern of seismicity in Southern California [24], as described in the text.

we only consider epicenters in the following. The catalog is assumed to be homogeneous from January 1984 to December 2002 and complete for events with magnitude larger than  $m_c = 2.5$  located within the rectangle  $(120.5^\circ W, 115.0^\circ W) \times (32.5^\circ N, 36.0^\circ N)$  [42]. Restricting ourselves to magnitudes larger than  $m_c$  gives  $N = 22217$  events (see Fig. 3). In order to test for robustness and the dependence on magnitude, we analyze this sub-catalog and subsets of it, obtained in two different ways: By (a) selecting different threshold magnitudes, namely  $m = 3.0, 3.5, 4.0$  giving  $N = 5857, 1770$  and  $577$  events, respectively, or (b) using a shorter period from January 1984 to December 1987 giving  $N = 4744$  events for magnitude threshold  $m = m_c$ .

It is important to note that all events in the catalog are treated in the same way. In particular, we do not distinguish between foreshocks, mainshocks and aftershocks. Hence, our definition of a recurrence – an event is a recurrence of any previous event if it is closer to it in space than all the intervening events – is *a priori* independent of those classifications. Note also that our definition of a recurrence is wholly unrelated to the notion of “characteristic earthquakes” on a single fault as introduced, for example, in Refs. [43, 44, 45].

Fig. 4 shows the recurrences with magnitude  $m \geq m_c$  defined by our method for one randomly chosen event in the catalog, an earthquake of magnitude 2.9 that oc-

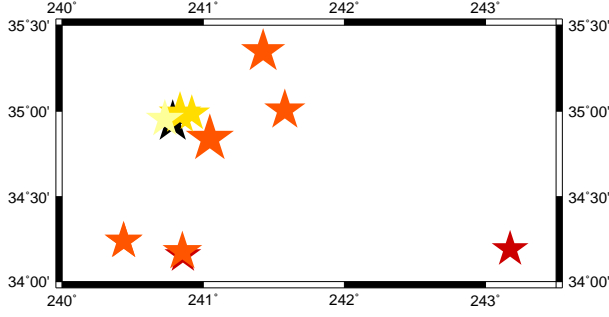


FIG. 4: (Color online) Map showing a 2.9 earthquake (black) and its recurrences as defined by our method. The size of the symbols linearly scales with the magnitude of the event and its color corresponds to the time of occurrence (from darker colors to lighter colors). See Table I for more details.

TABLE I: List of recurrences of the 2.9 earthquake given in Fig. 4 as defined by our method for threshold magnitude  $m = 2.5$ .

rank	magnitude	$l$ (km)	$T$ (h)
1	2.5	234.36	22.16
2	2.5	87.39	42.81
3	2.7	84.98	198.87
4	2.5	84.34	232.94
5	2.6	83.97	236.56
6	3.0	73.99	296.51
7	2.8	72.80	424.95
8	3.3	26.37	961.64
9	2.5	13.38	3471.73
10	2.9	6.99	3482.97
11	2.6	5.31	25452.30

curred on January 10, 1999. The actual spatial and temporal distance between this event and each of its recurrences is listed in Table I. It has to be noted that the number of recurrences of a given earthquake or Event-0 is generally not related to its magnitude. The number of recurrences of the largest earthquakes like the Landers event or the Hector mine event are just above the average (see Section IV B). Thus, most recurrences are associated to Event-0s with small magnitude — which are much more abundant according to the Gutenberg-Richter law.

#### A. Spatial distances of recurrences

Fig. 5 shows the estimated PDF  $p^m(l)$  of recurrences at a spatial distance  $l$  in the sub-catalog with threshold magnitude  $m$ . The PDFs exhibit a peak at a typical

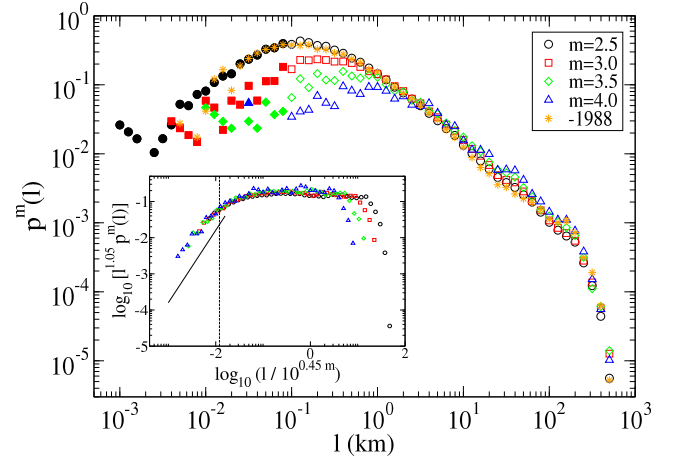


FIG. 5: (Color online) Distribution of distances  $l$  of recurrent events for sets with different magnitude thresholds  $m$ . The distribution for  $m = 2.5$  up to 1988 is also shown and is almost indistinguishable from the data for the full catalog with  $m = 2.5$  — showing the invariance of the distribution with respect to the time span of the recorded events. Filled symbols correspond to distances below 100 m and are unreliable due to location errors. The inset shows a data collapse, obtained by rescaling distances and distributions according to Eq. (53) (excluding unreliable points). The full straight line has slope 2.05; the vertical dashed line indicates the pre-factor  $L_0$  in the scaling law for the characteristic distance,  $l^*(m) = L_0 \times 10^{0.45m}$ . Note that  $\int_0^\infty p^m(l) dl = 1$ .

distance,  $l^*(m)$ , which increases with magnitude. For sufficiently large  $l$ , all distributions show a power law decay with an exponent  $\approx 1.05$  up to a cutoff. This cutoff corresponds to the size of the region in Southern California that we consider, and hence is a finite size effect. For small distances  $l < l^*(m)$ , we observe an approximately linear increase.

With a suitable scaling ansatz, the different curves in Fig. 5 fall onto a universal curve, except at the finite size cutoff. The inset in Fig. 5 shows results of a data collapse using

$$p^m(l) \approx l^{-1.05} F(l/10^{0.45m}). \quad (53)$$

The scaling function  $F$  has two regimes, a power-law increase with exponent  $\approx 2.05$  for small arguments and a constant regime at large arguments. The transition point between the two regimes can be estimated by extrapolating them and selecting the intersection point, giving  $L_0 = 0.012\text{km}$ . For the characteristic distance that appears in  $F$  we find

$$l^*(m) \approx L_0 \times 10^{0.45m}. \quad (54)$$

#### 1. Discovery of Causal Structure

Although  $p^m(l)$  has the same overall shape as the distribution  $p(l)$  of the finite null model (see Eq. (22)), there

are fundamental differences with respect to the dependence on the time span over which events are recorded. For the earthquake data,  $p^m(l)$  and in particular  $l^*(m)$  do not depend on the time span at all but rather depend directly on  $m$ . This conclusion comes from the explicit comparison of two different observation periods in Fig. 5 with the same  $m$ . With the exception of the smallest values of  $l$ ,  $p^{2.5}(l)$  is largely unaltered if only the sub-catalog up to 1988 is analyzed and  $l^*$  does not change at all. It is important to note that the total number of events in the latter sub-catalog is roughly 5 times smaller.

In the null model  $l^*$  depends explicitly on the finite time span of the observation period,  $T$ , as shown in Eq. (24). In the real data though, the spatiotemporal ordering of earthquakes determines the value of  $l^*$ , regardless of the duration of the observation period – as long as it is large enough to obtain sufficient statistics to determine  $l^*(m)$  and small enough that seismic correlations do not disappear over that time span. This is confirmed by analyses of other sub-catalogs (not shown). On this basis, we conclude that the characteristic length must therefore reflect robust physical properties of the underlying dynamics over the given observation periods. Its (quasi)-invariance is not a property of the null model. Therefore, it reflects causal structure in the dynamics of seismicity. As a result, if one re-arranges the seismic catalog by “shuffling” the locations and magnitudes of events (see Section IV B 1), then the invariance of  $l^*$  is lost and the distribution of recurrences behaves the same as the null model for spatial dimension  $D = 2$  (see Eqs. (22,24)). To sum up: the invariance of  $l^*(m)$  is an indicator of causality and is thereby a physically meaningful length scale in the dynamics of seismicity over the time scales we can explore with statistical methods – minutes to decades.

## 2. Identification with the Rupture Length

The almost complete lack of dependence of  $p^m(l)$  (excluding very small values of  $l$ ) on the considered time span can be explained by at least two scenarios: 1) Recurrences with  $l \ll l^*(m)$  are greatly *suppressed* at large time scales; 2) Recurrences with  $l \approx l^*(m)$  are greatly *enhanced* at short time scales compared to the null model with *constant* rate. As we will discuss below, it is likely that both effects are present.

Physically, such a behavior is reasonable if we identify  $l^*$  with the rupture length of the earthquake that starts a chain of recurrences. As described by Omori’s law [46], the rate of seismic activity tends to increase directly after an earthquake nearby (close to the rupture area of the event). Moreover, there is some evidence that due to the stress relief within the rupture area itself, it tends to exhibit less seismic activity for awhile — see, for example, Ref. [47]. This supports the hypothesis that activity increases for  $l \approx l^*(m)$  at shorter times, but gets suppressed for  $l \ll l^*(m)$  over longer times.

This identification is also affirmed by the fact that the scaling of  $l^*(m)$  with  $m$  is close to the estimated behavior of the rupture length  $L_R(m') \approx 0.02 \times 10^{m'/2}$  km given in Ref. [48] and remarkably close to  $L_R(m') = \sqrt{A_R} \approx 0.018 \times 10^{0.46 m'}$  km given in Ref. [49], where  $m'$  is the magnitude of the earthquake and  $A_R$  its rupture area. The close agreement between the latter and Eq. (54) suggests that the characteristic length scale of distances for recurrent events is indeed the rupture length of events with  $m' = m$ , defined in terms of the rupture area  $l^* = L_R \equiv \sqrt{A_R}$ . Thus, our approach allows us to discover the rupture length as a causal consequence of the dynamics based purely on the spatiotemporal organization of seismicity without any additional knowledge of the microscopic dynamics and the actual rupture processes that occur – even, in fact, treating the seismic events as point-like in space and time!

The identification  $l^* = L_R$  is also consistent with the fact that the description of earthquakes as a point process breaks down below the rupture length. Then, the relevant distance(s) between earthquakes is not determined solely by their epicenter positions but also by the relative orientation and size of the extended ruptures in 3D space. Thus, we expect to find a different correlation structure for distances smaller than the rupture length. In fact, this is precisely what our data show, namely a linear increase at small distances,  $l \ll l^*(m)$  (see the main part of Fig. 5 and also the straight line with a slope of 2.05 in the inset of Fig. 5).

## 3. Robustness of $l^*(m)$

The lengths  $l^*$  observed for the values of  $m$  we consider are larger than the location errors ( $\approx 100$  m). Simulations show that  $p^4(l)$  (blue triangles in Fig. 5) does not change substantially if the epicenters in the catalog are randomly relocated by a small distance up to one kilometer. Yet, the maximum for  $p^{2.5}(l)$  shifts to larger  $l$  with this procedure, destroying the scaling of  $l^*(m)$ . Since the smallest  $l^*$  that obeys the data collapse is  $\approx 160$  m, the data collapse we observe for the original data verifies that the relative location errors are indeed less than 100 m, or of that order [50]. Furthermore, the absence of any anomaly due to location errors near 100 m in Fig. 5 indicates that recurrences within the rupture area lack correlations. This is also supported by Eq. (22) which predicts the observed behavior  $p^m(l) \propto l$  for  $l < l^*$  if events are happening uniformly and randomly in 2D space during a finite observation period, or are recorded as happening randomly in space due to location errors.

## 4. Spatial Hierarchy of Subsequent Records

To further examine the behavior of  $p^m(l)$ , we study separately the contributions of recurrences with definite rank. The rank  $i$  is defined as in Sec. III F, i.e., for a

given Event-0, recurrence  $i+1$  directly follows recurrence  $i$  as shown in Fig. 2. Since  $p^m(l)$  is the PDF that *any* recurrence occurs at distance  $l$  for a catalog with threshold magnitude  $m$ , we have for any finite number of events  $N$ ,

$$p^m(l) = \sum_{i=1}^{N-1} p_{rec}(i) p_i^m(l) = \frac{\sum_{i=1}^{N-1} N_i p_i^m(l)}{\sum_{i=1}^{N-1} N_i}, \quad (55)$$

where  $p_{rec}(i)$  is the probability that a randomly chosen recurrence is an  $i$ 'th recurrence,  $N_i$  is the number of events in the sequence that have at least  $i$  recurrences (or out-going links), and  $p_i^m(l)$  is the conditional PDF that, given that a recurrence is an  $i$ 'th recurrence, it happens at distance  $l$ .

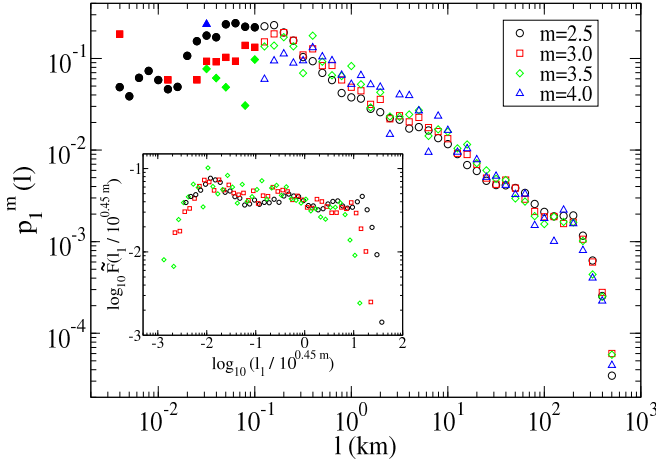


FIG. 6: (Color online) Distribution of distances  $l$  of the *first* recurrence for different magnitude thresholds  $m$ . Filled symbols correspond to distances below 100 m and are unreliable due to location errors. Note that  $\int_0^\infty p_1^m(l) dl = 1$ . Inset: Data collapse obtained by rescaling distances and distributions according to Eq. (56) (excluding unreliable points).

In the inset of Fig. 6, the data are analyzed according to the *ansatz* that the distribution of first recurrences,  $p_1^m(l)$ , has the scaling form

$$p_1^m(l) = l^{-\delta_r} \tilde{F}(l/10^{0.45} m), \quad (56)$$

with  $\delta_r \approx 0.6$  and  $\tilde{F}$  similar to  $F$  (see Eq. (53) and the inset of Fig. 5 for comparison). In particular, the same characteristic distance  $l^*(m)$  appears as for  $p^m(l)$ . Moreover, we find that the latter is true for all  $p_i^m(l)$  — which is further evidence supporting the interpretation of  $l^*$  as the rupture length. The behavior of  $p_1^m(l)$  indicated in Fig. 6 and described by Eq. (56) extends earlier results for a catalog from Southern California with lower spatial resolution ( $\approx 1$  km) which did not allow to resolve the dependence on  $m$  [35].

Related to the distribution of distances for recurrent events is the distribution of distance ratios  $l_{i+1}/l_i$  of consecutive recurrences. Here again recurrences are ordered such that recurrence  $i+1$  directly follows recurrence  $i$ . For  $i = 0$ , we take  $l_0 = 634.3$  km, which is the largest

possible distance in the region covered by the catalog. By construction these ratios are always between zero and one. We denote by  $q_i^m(x)$  the PDF that  $l_{i+1}/l_i = x$  for each event that has an  $(i+1)^{th}$  recurrence. As indicated in Fig. 7, the data for  $m = 2.5$  and  $i = 0$  (black circles) scale over a wide region as  $q_0^{2.5}(x) \sim x^{-\delta_r}$  with  $\delta_r \approx 0.6$ . This is expected since  $q_0^m(x) \sim p_1^m(l)$ . Although each distribution  $q_i^{2.5}(x)$  is different, the curves for  $i \geq 1$  also show (more restricted) power law decay comparable to  $q_0^{2.5}(x)$ . For  $l_{i+1}/l_i \rightarrow 1$  they also exhibit a peak that becomes more pronounced with increasing  $i$ . This is due to recurrences occurring at almost the same distance (but not at the same place!) suggesting again that recurrences are suppressed within the rupture area, but are enhanced just outside that area.

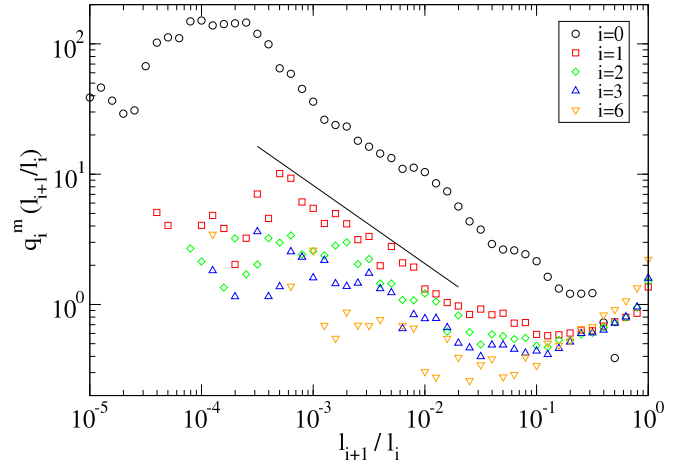


FIG. 7: (Color online) Distribution of recurrence distance ratios  $l_{i+1}/l_i$  for  $m = 2.5$  and different values of  $i$  with  $l_0 = 634.3$  km. The straight line corresponds to a decay with exponent 0.6. Note that  $\int_0^\infty q_i^m(x) dx = 1$ .

The observed behavior of  $q_i^{2.5}(x)$  and  $p_1^m(l)$  is very different from the behavior predicted by the null model. For the null model, in the long time limit, Eq. (44) gives  $q_i^m(x) = D x^{D-1}$  which is not only independent of  $i$  but also purely determined by the spatial dimension  $D$  — and is increasing for  $D > 1$  rather than decreasing. Similarly, Eq. (43) gives  $p_1^m(l) \propto l^{D-1}$  for the null model. For Southern California, it has been found that  $D = D_2 = 1.2$  [35, 36], which would lead to an increasing function  $q_i^m(x) \sim x^{0.2}$  rather than a decaying power law behavior. Although the above predictions of the null model are only strictly true in the infinite time limit, we point out that repeating this analysis of the hierarchy of recurrences for a “shuffled” catalog reveals behavior in close agreement with the null model and diametrically opposed to the results shown in Fig. 7 for the actual seismic record [36].

Thus, the observed behavior of  $q_i^{2.5}(x)$  and  $p_1^m(l)$  as well as the value of  $\delta_r$  are *not* determined by the spatial distribution of seismicity alone but reflect causal structures leading to the complex *spatiotemporal* organization

of seismicity. Moreover, the shape of  $p_1^m(l)$  shows that the first recurrence is much more likely to happen at a typical distance of  $l^*$  than predicted by the null model. This enhancement goes along with a suppression of recurrences with  $l \ll l^*$  as the increasing (with  $i$ ) peak at  $x = 1$  for  $q_i^m(x)$  indicates. These results support the overall picture that recurrences with  $l \ll l^*(m)$  are greatly *suppressed* at large time scales while recurrences with  $l \approx l^*(m)$  are greatly *enhanced* at short time scales.

## B. Network properties

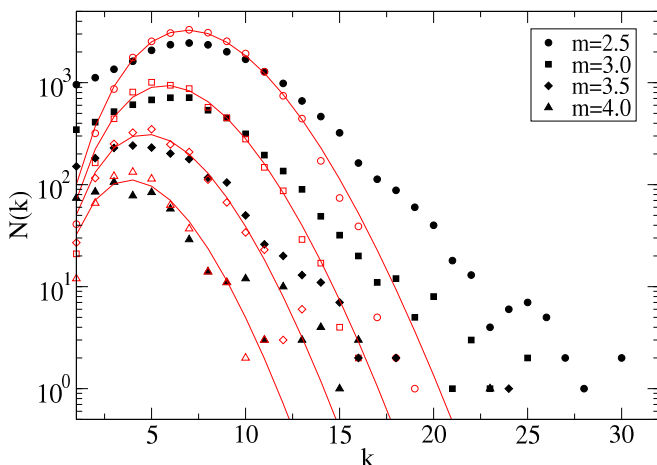


FIG. 8: (Color online) In- and out-degree histograms for different values of  $m$ . For a given earthquake, the in-degree (out-degree)  $k$  is the number of links directed at it (originating from it) as defined in Section II. Open (red) symbols correspond to the in-degree, filled (black) symbols correspond to the out-degree. Error bars can be estimated as  $\sqrt{N(k)}$ . The red lines correspond to Poisson distributions with the same respective mean and normalization.

We now turn to the analysis of seismicity in terms of the statistical properties of its network of recurrences (or records) as defined in Section II and illustrated in Fig. 1. Fig. 8 shows the in- and out-degree histograms for different values of  $m$ , which are compared to Poisson distributions with the same respective mean degree and normalization ( $\langle k \rangle = 7.40, 6.24, 5.20, 4.35$  for  $m = 2.5, 3.0, 3.5, 4.0$ , respectively). A Poisson out-degree and in-degree distribution is expected for the null model (see Eq. (47) and Eq. (50)). For the actual seismic network, the out-degree distributions are significantly different from a Poissonian [51]. In particular, the network keeps a preponderance of nodes with small out-degree as well as an excess of nodes with large out-degree compared to a Poisson distribution. This effect becomes more pronounced with increasing magnitude.

The behavior of the out-degree distribution implies that the network topology is able to discern consequences of the causal structure of seismicity: The preponderance

of nodes with small out-degree, for example, can be related to the physical picture discussed above that seismic activity is typically greatly enhanced directly after the occurrence of an earthquake close to its rupture area but suppressed within the rupture area itself. Such a dynamics makes it more likely that only very few recurrences occur, even at long times. For the in-degree distributions, we find that they roughly agree with a Poisson distribution although there are still significant deviations from the null model for  $k = 1$  [52].

Note, however, that  $\langle k \rangle$  — which is obviously the same for the in- and out-degrees — decreases with  $m$ , simply because the number of events  $N$  shrinks with  $m$ . This is shown in Fig. 9 where  $\langle k \rangle$  is also displayed for a randomly shuffled catalog.

### 1. Shuffling Procedure

Shuffling was performed in the following way: Consider all events in the catalog with magnitude  $m' \geq m_c = 2.5$ . Shuffle the magnitudes and the epicenter locations separately, keeping the times of occurrence, and then apply the recurrence analysis for the different subsets defined by different magnitude thresholds as before. The shuffled catalog can, thus, be considered as a realization of a random process with no spatiotemporal correlations, although both spatial correlations and temporal correlations may persist separately. Based on the null model and Eq. (47), we expect a Poisson out-degree distribution with  $\langle k \rangle \approx \ln N$  which is exactly what we find for the randomly shuffled catalog. This dependence of  $\langle k \rangle$  can be clearly seen in Fig. 9. Yet, for the original earthquake data we find for large  $N$

$$\langle k \rangle \approx 0.8 \ln N. \quad (57)$$

Hence, the average number of recurrences is significantly less than for the null model, which is presumably related to the suppression of recurrences with  $l < l^*(m)$  — as discussed earlier. Fig. 9 gives further evidence that recurrences emphasize particular aspects of spatiotemporal clustering, associated with the causal dynamics of seismicity.

### 2. Degree-degree Correlations

The causal structure of seismicity does not, however, induce strong degree-degree correlations between events and their recurrences other than those arising from the temporal order of a finite sequence of events — as in the acausal null model. Panels A to C in Fig. 10 show the average out-degree and in-degree of recurrences as a function of the in-degree or out-degree of their corresponding Event-0 [53]. There are no qualitative differences between the actual earthquake catalog from California and a surrogate, which is a randomly shuffled version of the

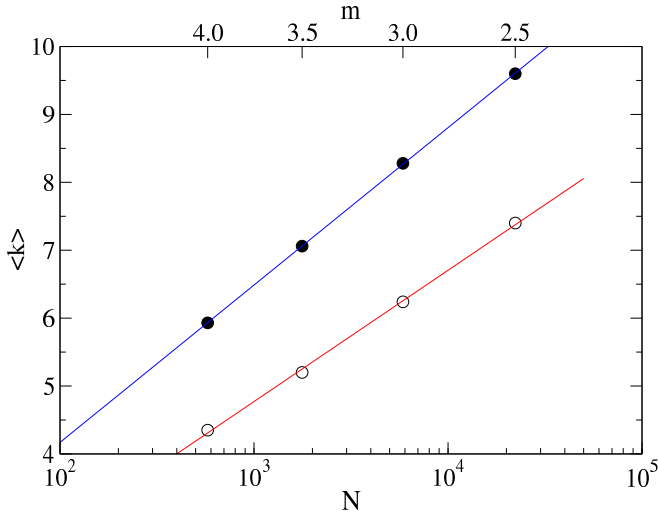


FIG. 9: (Color online) Mean degree  $\langle k \rangle$  as a function of number of events  $N$  (or magnitude  $m$ ). Open symbols correspond to the original catalog for different values of  $m$ , while filled symbols correspond to the shuffled catalog (see text). The lines correspond to best fits giving  $\langle k \rangle_{\text{original}} = -1.03 + 0.84 \ln N$  and  $\langle k \rangle_{\text{shuffled}} = -0.47 + 1.01 \ln N$ .

catalog. In particular, the behavior shown in panel A and B agrees with the acausal null model (see discussion following Eq. (52)). Note that the offset between the two data sets is simply due to different  $\langle k \rangle$ .

The situation is different for the dependence of the mean out-degree on the in-degree of the *same* node. As shown in Eq. (52),  $\langle k^{\text{out}} \rangle$  has a weak dependence on  $k^{\text{in}}$  in the null model such that  $\langle k^{\text{out}} \rangle$  decreases with  $k^{\text{in}}$ . This is exactly what we find for the shuffled catalog as shown in panel D of Fig. 10. However, the same panel also shows that for the actual earthquake catalog  $\langle k^{\text{out}} \rangle$  increases with  $k^{\text{in}}$  – exactly the opposite of the null model. Moreover,  $k^{\text{in}} < \langle k \rangle$  implies  $k^{\text{out}} < \langle k \rangle$  on average. This is again consistent with a causal dynamics where earthquakes are clustered in space and time.

### 3. Clustering coefficient

Other network properties include various measures of clustering. In general terms, clustering quantifies how well connected the neighbors of a node are among themselves. In the case of recurrences, it refers to the likelihood that recurrences of the same event are also recurrences of each other. There are different, inequivalent definitions of the clustering coefficient  $C$  [54]. Here we focus on the definition based on the local clustering coefficient  $C_i$  adapted to directed networks.

For all nodes  $i$  with out-degree larger than one, the clustering coefficient  $C_i$  is given by the ratio of existing links  $E_i$  between its  $k_i^{\text{out}}$  recurrences to a possible number of such links,  $\frac{1}{2}k_i^{\text{out}}(k_i^{\text{out}} - 1)$ . Then the clustering coefficient  $C$  of the network is defined as the average over

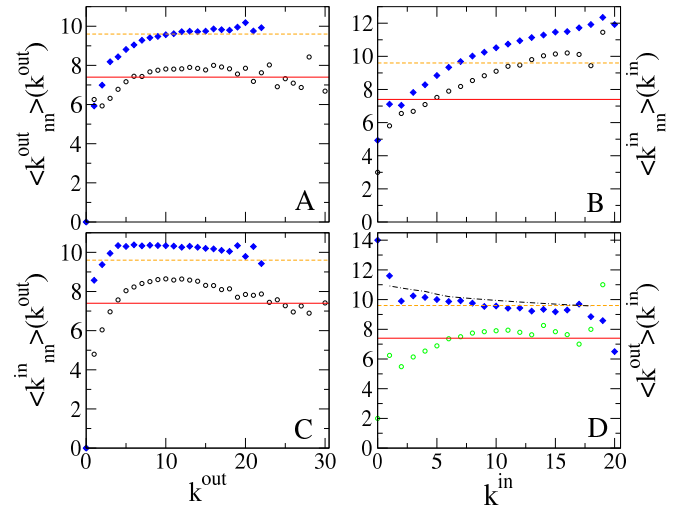


FIG. 10: (Color online) Panels A – C: degree correlations between the Event-0 and its recurrences. The average in-degree  $\langle k_{nn}^{\text{in}} \rangle$  or out-degree  $\langle k_{nn}^{\text{out}} \rangle$  of the recurrences of all nodes with a given in-degree  $k^{\text{in}}$  or out-degree  $k^{\text{out}}$  for  $m = 2.5$  is shown. Open (black) circles correspond to the original earthquake catalog from California, filled (blue) diamonds correspond to the shuffled catalog. The mean degree is indicated by the (red) solid line and the (orange) dashed line, respectively. Panel D shows the average out-degree of a node as a function of its in-degree. Open (green) circles correspond to the original earthquake catalog from California, filled (blue) diamonds correspond to the shuffled catalog. The black dash-dotted line is the approximation for the null model given in Eq. (52). In this panel, the behavior of the original earthquake data is qualitatively very different from the null model and the shuffled catalog.

all nodes  $i$  with out-degree larger than one

$$C = \langle C_i \rangle = \left\langle \frac{2E_i}{k_i^{\text{out}}(k_i^{\text{out}} - 1)} \right\rangle_i. \quad (58)$$

This definition implies, for example, that the clustering coefficient of an Erdős-Rényi graph is equal to the probability of linking each pair of nodes,  $p_{\text{link}} = \langle k \rangle / (N - 1) = C_{\text{rand}}$ .

For the data from California, we obtain  $C = 0.2647$  for  $m = 2.5$ . This is significantly larger than  $C = 0.1825$ , which is the value for the shuffled catalog. It has to be pointed out, though, that the average is performed over a different number of nodes in the two cases since the shuffled catalog hardly contains any events with out-degree equal to one. For the shuffled catalog, there are only 15 events with  $k^{\text{out}} = 1$ , which is close to the expected value of 10.6 for the random model – see Eq. (48). This value is two orders of magnitude less than for the actual seismic data.

Another difference between the two data sets is the distribution of  $C_i$ . For the actual earthquake data, the distribution is much broader. The standard deviation for the distribution is 0.2146 compared to 0.0934 for the shuffled catalog. This difference is mainly due to the fact



that the original data contain many events with  $C_i = 0$  or  $C_i = 1$  – unlike the shuffled catalog.

### C. Temporal distances of recurrences

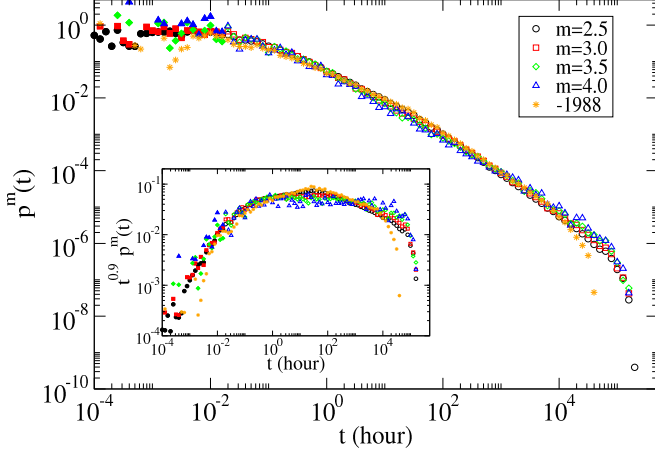


FIG. 11: (Color online) Distributions of the waiting times between Event-0s and their recurrences for the original catalog and different threshold magnitudes  $m$ . The distribution for  $m = 2.5$  up to 1988 is also shown. Filled symbols correspond to times below 90 seconds which are underestimated and unreliable due to measurement restrictions: The finite rupture times of earthquakes and the associated seismic coda, which consists of a superposition of incoherent scattered waves, place limitations on the identification and separation of earthquakes. The inset shows the rescaled distributions. Note that  $\int_0^\infty p^m(t) dt = 1$ .

The temporal distances between events and their recurrences can be analyzed in the same way as the spatial distances. The PDF  $p^m(t)$  for these waiting (or “inter-occurrence”) times for different threshold magnitudes  $m$  is shown in Fig. 11. These all decay roughly as  $1/t^\alpha$  with  $\alpha \approx 0.9$  for intermediate times as indicated in the inset. The apparent scaling region in Fig. 11 shows some curvature, though. Due to the finite duration of the catalog, there is an observational cut-off at the longest time scales. At the shortest time scales,  $p^m(t)$  goes over to a constant limit. While the shape of the distribution is roughly similar to the null model (see Eq. (23)),  $p^m(t)$  for the earthquake catalog is *independent* of  $m$  and, hence, the number of events in the catalog. This invariance is (again) drastically at odds with the null model where the temporal rate  $\Lambda = abR^D$  determines the transition point and  $\Lambda$  itself depends on the number of events  $N$  as shown in Eqs. (25,27).

As described in what follows, the analysis for the shuffled catalog shown in Fig. 12 is consistent with the acausal null model. As predicted by the null model, the distributions for the shuffled catalog must be rescaled by the rate of events in order to obtain a data collapse. Furthermore, the invariant behavior (with respect to mag-

nitude  $m$ ) we observe for recurrences in the original catalog differs substantially from earlier results for waiting time distributions between subsequent earthquakes [36, 37, 38, 39]. It reflects a new non-trivial feature of the spatiotemporal dynamics of seismicity that appears when events other than the immediately subsequent ones – used to conventionally define waiting times – are considered.

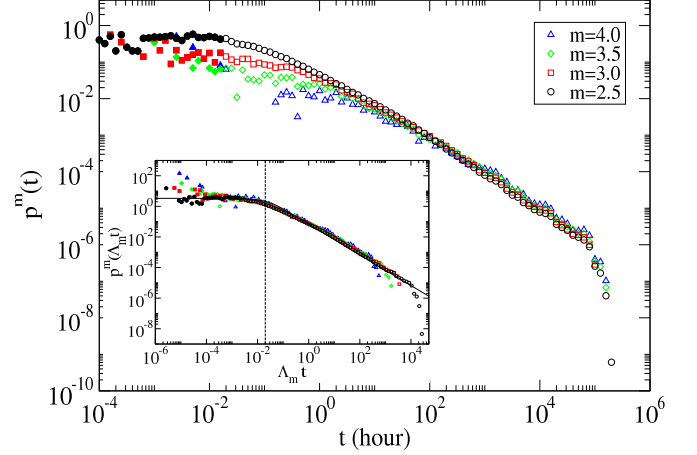


FIG. 12: (Color online) Distributions of the waiting times between Event-0s and their recurrences in the shuffled catalog (see text) for different threshold magnitudes  $m$ . Filled symbols correspond to times below 90 seconds which are underestimated and unreliable. The inset shows the distributions rescaled by the respective rate of events  $\Lambda_m$ . The solid line corresponds to a best fit assuming the functional form given in Eq. (23). The dashed line highlights the transition point between the constant behavior and the  $1/t$  decay. Note that  $\int_0^\infty p^m(t) dt = 1$ .

For the shuffled catalog,  $p^m(t)$  closely follows the theoretical prediction of Eq. (23) and in particular the dependence on  $m$  – or rather on  $N$  through  $\Lambda$ . As shown in the inset of Fig. 12, the different distributions — with the obvious exception of the observational cut-off at the largest time scales — collapse onto a single curve if  $t$  is rescaled by the respective rate  $\Lambda_m$ . Here,  $\Lambda_m$  is the mean rate of earthquakes above magnitude threshold  $m$  for the observation period. Notably, the main deviation from the *stationary* null model is that the location of the transition point for the shuffled catalog is not at  $\Lambda_m t = 1$  but rather at  $\Lambda_m t = 0.02$ . This is expected and due to the fact that the rate of seismic activity — which is preserved in the shuffled catalog — is *not* constant over time but exhibits large, correlated fluctuations as indicated, for example, by Omori’s law [46].

The relative times between subsequent recurrences in the hierarchy can be analyzed in the same way as distances were in Sec. IV A 4. Fig. 13 shows the PDFs for the ratios  $t_i/t_{i+1}$  for subsequent recurrences, i.e., recurrences are ordered such that recurrence  $i + 1$  directly follows recurrence  $i$ . For the cases shown, two power-law regimes seem to exist: For arguments smaller than about

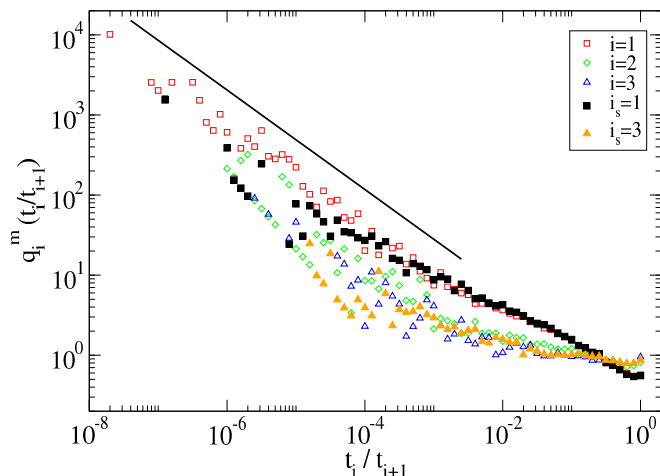


FIG. 13: (Color online) Distribution of waiting time ratios  $t_i/t_{i+1}$  for  $m = 2.5$ . The straight line has slope  $-0.62$ . Open symbols correspond to the original earthquake catalog, filled symbols to the shuffled catalog (see text). Note that  $\int_0^\infty q_i^m(x)dx = 1$ .

$10^{-3}$ ,  $q_i^{2.5}(t_i/t_{i+1})$  decays with an exponent  $\delta_t \approx 0.6$  roughly independent of  $i$ , for larger arguments the decay is slower and the exponent apparently decreases further with  $i$ . Clearly, the broadest scaling regime materializes for  $t_1/t_2$ .

The behavior of  $q_1^{2.5}(t_1/t_2)$  for  $10^{-3} < t_1/t_2 \ll 1$  could be compared to Eq. (38), although the latter was derived for the translational invariant case. Equally important, Eq. (38) only holds for the *stationary* null model. As discussed above, seismic activity is *not* constant over time but exhibits large fluctuations. Fig. 13 shows that these fluctuations as well as the loss of translational invariance are responsible for the behavior for arguments larger than about  $10^{-3}$ , since there is no observed difference between the original and the shuffled catalog. Yet, the deviations between the original data and the shuffled catalog for smaller arguments indicate that those short time differences arise from the causal spatiotemporal organization of seismicity.

#### D. Discussion

It is important to discuss our results for the network of recurrences (or records) in view of what is known about causal connections between earthquakes. One specific type of causal connection is earthquake triggering. The increased seismic activity following large earthquakes — as described by the Omori law [46] leading to the identification of aftershocks — is the most obvious example of earthquakes being triggered in part by preceding events. Aftershock sequences of small earthquakes are less obvious because the aftershock productivity is weaker, but can be observed after stacking many sequences [55]. Other approaches [16, 25] have generalized

the definition of an aftershock so that an event can be an aftershock of more than one event leading to networks of earthquakes and aftershocks. Earthquake triggering is typically associated with stress changes which can be static stress changes imparted by the preceding shock or dynamic stress changes associated with seismic wave propagation or combinations of them as discussed, for example, in Refs. [56, 57, 58, 59, 60]. The proposed physical mechanisms to explain earthquake triggering due to *static* stress change induced by a prior event include rate-and-state dependent friction [61], crack growth [62, 63, 64], viscous relaxation [65], static fatigue [66], pore fluid flow [67], and simple sandpile models [68].

Calculations of stress changes have been used to predict the locations, focal mechanisms and times of future earthquakes (see Refs. [56, 57, 69] for reviews). The success of this method is limited. Only about 60% of aftershocks are located where the stress increased after a main shock [70]; stress shadows are seldom or never observed [71, 72]; and the correlation of stress change with aftershocks is rather sensitive to the assumed slip distribution [73]. All of this could be due to the fact that most studies have neglected the influence of small earthquakes and secondary aftershocks which can play an important role [55, 74]. Moreover, most studies have also neglected the influence of *dynamic* stresses radiated by seismic waves from (small or medium-sized) earthquakes which may also play an important role — even in the near field (see, e.g., Refs. [75, 76, 77, 78, 79, 80]). In particular, dynamic stress changes can dominate the triggering mechanism over a wide range of distances between 0.2 and 50 kilometers from the fault rupture [81].

While it is not entirely clear how our results for the network of recurrences could allow one to distinguish between the different types of stress changes associated with earthquake triggering, there are a number of currently unexplained observations that could be related to a particular triggering mechanism. The excess of events with a large number of recurrences compared to the null model (see Fig. 8) is one of them. Other examples include the correlations between the in-degree and the out-degree of a given event (see Fig. 10 D) and the apparent invariance of the waiting time distribution with respect to the threshold magnitude (see Fig. 11). The sensitivity of these properties as well as our other findings (especially the invariance of  $l^*(m)$  with respect to the time span) to the triggering mechanism can be tested within the framework of the “epidemic type aftershock sequence” model which has been established as an improved stochastic null model for seismicity [82, 83]. It allows one to vary the spatial scaling of the triggered events depending on the assumed underlying triggering mechanism, namely static stress changes or dynamic stress changes [81, 84]. This will be the topic of a future publication.

Finally, we would like to point out that simple and direct comparisons of our results for the network of recurrences (or records) with known results for aftershocks are not justified. This is due to the fact that recurrences



as defined by our method are at best a very small and *non-random* subset of what typically would be considered the set of aftershocks. Also, the power-law decay of the distribution of distances as shown in Fig. 5 occurs generically for a wide class of processes due to the properties of records as discussed in Section III — independent of the specific properties of aftershock sequences described, for example, in Ref. [81]. Similarly, the power-law decay of the distribution of waiting times (see Fig. 11) is also a generic property of records as discussed in Section III and is, thus, not related to the specific characteristics of aftershock sequences discussed in Refs. [85, 86].

## V. SUMMARY

This paper provides a method to detect features in a temporal sequence of observations that can be plausibly attributed to causal dynamics even when the observer has no *a priori* knowledge of the underlying dynamics. Our starting point is to generalize the concept of a recurrence for a point process in time to recurrent events in space and time. An event is defined to be a recurrence of any previous event if it is closer to it in space than all the intervening events; i.e. if it constitutes a record breaking event. Hence, the causal structure of events may be described as a network of events linked to their recurrences. Each event can have many previous events pointing to it (its potential causes) and many future events (its effects). Causality can be plausibly inferred when the statistical properties of the network constructed using this method and the statistics of the records deviate strongly from those resulting from almost any acausal process.

We derive analytically many properties for the network of recurrent events composed by random processes in space and time. In doing so, we develop a fully symmetric theory of records where both the variable in which records occur and time, itself, are continuous. This simplifies the theory and in our view makes it more elegant. We discover a number of new analytic results for record breaking statistics.

Many of those results are compared to properties of the network synthesized from time series of epicenter locations for earthquakes in Southern California. Significant disparities that can be attributed to causality are

mainly coming from the invariance of network statistics with the time span of the events considered. This is presumably related to an observed hierarchy in the distances and times of subsequent recurrences. As a result a fundamental length scale for recurrences is obtained solely from the earthquake epicenter data, which can be identified as the rupture length. All these significant deviations disappear when the analysis is repeated for a surrogate in which the original magnitudes and locations of earthquake epicenters are randomly “shuffled”. Almost all of the latter results are completely consistent with predictions from the acausal null model. Taken together these results suggest that causality in seismic dynamics may be much broader than any normative interpretation of “triggering”.

Our results are generally robust with respect to modifications of the rules used to construct the network, e.g., using spatial neighborhoods such that the construction becomes symmetric under time reversal or taking into account magnitudes. All such modifications have the drawback that they do not define a record breaking process consisting of recurrences to each event. For seismicity, our results are also unaltered if we exclude unphysical links with propagation velocities larger than the velocity of a “P wave” of about  $6\text{km/sec}$  ( $\approx 0.1\%$  of all links). This is also true if we restrict ourselves to velocities smaller than the velocity of a shear wave of about  $3.5\text{km/sec}$  which is often thought to be more relevant.

By building certain specific features of causality into null models, it is possible to refine predictions and examine what features in the network of seismicity are due to those aspects of causality and what are yet to be explained. It remains to be seen how general our method may turn out to be. In principle it can be applied to any high resolution data set where events occur in space and time. Immediate applications may include analyses of other geophysical or astrophysical data sets, brain scans [87], or analyses of models to validate or falsify them.

## Acknowledgments

We thank the Southern California Earthquake Center (SCEC) for providing the data.

- 
- [1] P. J. Cote and L. V. Meisel, Phys. Rev. Lett. **67**, 1334 (1991).
  - [2] J. P. Sethna, K. A. Dahmen, and C. R. Myers, Nature **410**, 242 (2001).
  - [3] K. Nagel and M. Paczuski, Phys. Rev. E **51**, 2909 (1995).
  - [4] P. Bak, *How nature works* (Copernicus, New York, 1996).
  - [5] J. D. Farmer, D. E. Smith, and M. Shubik, Physics Today **58**, 37 (2005).
  - [6] P. Bak, K. Chen, and C. Tang, Phys. Lett. A **147**, 297 (1990).
  - [7] D. L. Turcotte, Rep. Prog. Phys. **62**, 1377 (1999).
  - [8] P. Bak and K. Sneppen, Physical Review Letters **71**, 4083 (1993).
  - [9] J. P. Crutchfield and P. Schuster, *Evolutionary Dynamics: Exploring the Interplay of Selection, Accident, Neutrality, and Function* (Oxford University Press US, NY, NY, 2003).
  - [10] B. Drossel, Advances in Physics **50**, 209 (2001).
  - [11] W. R. Softky and C. Koch, Neural Computation **4**, 643 (1992).

- [12] D. Hughes, M. Paczuski, R. O. Dendy, P. Helander, and K. G. McClements, Phys. Rev. Lett. **90**, 131101 (2003).
- [13] M. Paczuski and D. Hughes, Physica A **342**, 158 (2004).
- [14] D. L. Turcotte, *Fractals and Chaos in Geology and Geophysics* (Cambridge University Press, Cambridge, UK, 1997), 2nd ed.
- [15] S. Stein and M. Wyss, *An Introduction to Seismology, Earthquakes, and Earth Structure* (Blackwell Publishing, Oxford, UK, 2002).
- [16] M. Baiesi and M. Paczuski, Nonlin. Proc. Geophys. **12**, 1 (2005).
- [17] P. Bak, C. Tang, and K. Wiesenfeld, Phys. Rev. Lett. **59**, 381 (1987).
- [18] W. Marzocchi, L. Zaccarelli, and E. Boschi, Geophys. Res. Lett. **31**, L04601 (2004).
- [19] In fact this is the definition of the  $\epsilon$ -recurrence as discussed in Ref. [88].
- [20] A. Helmstetter, G. Ouillon, and D. Sornette, J. of Geophys. Res. **108**, 2483 (2003).
- [21] N. Glick, The American Mathematical Monthly **85**, 2 (1978).
- [22] V. B. Nevzorov, Theory Prob. Appl. **32**, 201 (1987).
- [23] V. B. Nevzorov, *Records: Mathematical theory*, vol. 194 of *Translations of Mathematical Monographs* (American Mathematical Society, Providence, Rhode Island, 2001).
- [24] The seismic catalog was obtained from <http://www.data.scec.org/ftp/catalogs/SHLK/>.
- [25] M. Baiesi and M. Paczuski, Phys. Rev. E **69**, 066106 (2004).
- [26] M. Baiesi, Physica A **360**, 534 (2006).
- [27] R. Albert and A.-L. Barabasi, Rev. Mod. Phys. **74**, 47 (2002).
- [28] M. E. J. Newman, SIAM Review **45**, 167 (2003).
- [29] J. Davidsen, P. Grassberger, and M. Paczuski, Geophys. Res. Lett. **33**, L11304 (2006).
- [30] A. Shreim, P. Grassberger, W. Nadler, B. Samuelsson, J. E. S. Socolar, and M. Paczuski (2006), to be published in Phys. Rev. Lett..
- [31] B. B. Mandelbrot, in *Fractal Geometry and Stochastics*, edited by C. Bandt, S. Graf, and M. Zähle (Birkhäuser Verlag, Basel, 1995).
- [32] P. Sibani, M. Brandt, and P. Alstrøm, Int. J. Mod. Phys. **12**, 361 (1998).
- [33] J. Krug and K. Jain, Physica A **358**, 1 (2005).
- [34] J. B. Rundle, D. L. Turcotte, R. Shcherbakov, W. Klein, and C. Sammis, Review of Geophysics **41**, 1019 (2003).
- [35] J. Davidsen and M. Paczuski, Phys. Rev. Lett. **94**, 048501 (2005).
- [36] J. Davidsen and C. Goltz, Geophys. Res. Lett. **31**, L21612 (2004).
- [37] P. Bak, K. Christensen, L. Danon, and T. Scanlon, Phys. Rev. Lett. **88**, 178501 (2002).
- [38] A. Corral, Phys. Rev. E **68**, 035102 (2003).
- [39] A. Corral, Phys. Rev. Lett. **92**, 108501 (2004).
- [40] P. Shearer, E. Hauksson, G. Lin, and D. Kilb, Eos Trans. AGU **84**, 46 (2003).
- [41] P. Shearer, E. Hauksson, and G. Lin, Bull. Seismol. Soc. America **95**, 904 (2005).
- [42] S. Wiemer and M. Wyss, Bull. Seismol. Soc. America **90**, 859 (2000).
- [43] D. P. Schwartz and K. J. Coppersmith, J. of Geophys. Res. **89**, 5681 (1984).
- [44] M. W. Stirling, S. G. Wesnousky, and K. Shimazaki, Geophys. J. Int. **124**, 833 (1996).
- [45] M. V. Matthews, W. L. Ellsworth, and P. A. Reasenberg, Bull. Seismol. Soc. America **92**, 2233 (2002).
- [46] F. Omori, Journal of College Science, Imperial University of Tokyo **7**, 111 (1894).
- [47] A. M. Rubin and D. Gillard, Journal of Geophysical Research **105**, 19095 (2000).
- [48] Y. Y. Kagan, Bull. Seismol. Soc. America **92**, 641 (2002).
- [49] D. L. Wells and K. J. Coppersmith, Bull. Seismol. Soc. America **84**, 974 (1994).
- [50] Note that a systematic dependence of the location error on magnitude has not been reported in the literature and is also not present in the catalog at hand. It is unlikely that the characteristic length we see ( $l^*(m)$ ) is merely an artifact due to location error growing with magnitude.
- [51] For  $m = 2.5$ , the hypothesis that the out-degree distribution is Poissonian is rejected by the  $\chi^2$ -test at the 99.5% significance level. Specifically, we find  $\chi^2_0 = 66.7 \times 10^3$  for 22 degrees of freedom.
- [52] For  $m = 2.5$ , the hypothesis that the in-degree distribution is Poissonian is rejected by the  $\chi^2$ -test at the 99.5% significance level. Specifically, we find  $\chi^2_0 = 88.7$  for 15 degrees of freedom.
- [53] The averages were performed over all *links* emanating from events with fixed in-degree or out-degree, respectively.
- [54] S. N. Soffer and A. Vázquez, Phys. Rev. E **71**, 057101 (2005).
- [55] A. Helmstetter, Y. Y. Kagan, and D. D. Jackson, J. Geophys. Res. **110** (2005).
- [56] R. A. Harris, J. Geophys. Res. **103**, 24347 (1998).
- [57] R. S. Stein, Nature (London) **402**, 605 (1999).
- [58] A. M. Freed, Ann. Rev. Earth Planet. Sci. **33**, 335 (2005).
- [59] I. Main, Nature (London) **441**, 704 (2006).
- [60] E. P. Mallman and M. D. Zoback, J. Geophys. Res. **112**, B03304 (2007).
- [61] J. Dietrich, J. Geophys. Res. **99**, 2601 (1994).
- [62] S. Das and C. H. Scholz, J. Geophys. Res. **86**, 6039 (1981).
- [63] B. E. Shaw, Geophys. Res. Lett. **20**, 907 (1993).
- [64] I. Main, Bull. Seismol. Soc. America **90**, 86 (2000).
- [65] T. Mikumo and T. Miyatake, Geophys. J. Royal Astr. Soc. **59**, 497 (1979).
- [66] C. H. Scholz, J. Geophys. Res. **73**, 1417 (1968).
- [67] A. Nur and J. R. Booker, Science **175**, 885 (1972).
- [68] S. Hergarten and H. J. Neugebauer, Phys. Rev. Lett. **88**, 238501 (2002).
- [69] G. C. P. King and M. Cocco, Adv. Geophys. **44**, 1 (2001).
- [70] T. Parsons, J. Geophys. Res. **107**, 2199 (2002).
- [71] D. Marsan, J. Geophys. Res. **108**, 2266 (2003).
- [72] K. R. Felzer and E. E. Brodsky, J. Geophys. Res. **110** (2005).
- [73] S. Steacy, D. Marsan, S. S. Nalbant, and J. McCloskey, J. Geophys. Res. **109** (2004).
- [74] K. R. Felzer, T. W. Becker, R. E. Abercrombie, G. Ekström, and J. R. Rice, J. Geophys. Res. **107**, 2190 (2002).
- [75] D. Kilb, J. S. Gombert, and P. Bodin, Nature (London) **408**, 570 (2000).
- [76] J. S. Gombert, P. Bodin, and P. A. Reasenberg, Bull. Seismol. Soc. America **93**, 118 (2003).
- [77] D. Kilb, J. Geophys. Res. **108**, 2012 (2003).
- [78] T. Parsons, Geophys. Res. Lett. **32**, L04302 (2005).
- [79] P. A. Johnson and X. Jia, Nature (London) **437**, 871 (2005).
- [80] F. F. Pollitz and M. J. S. Johnston, Geophys. Res. Lett.

- 33**, L15318 (2006).
- [81] K. R. Felzer and E. E. Brodsky, *Nature (London)* **441**, 735 (2006).
  - [82] Y. Y. Kagan and L. Knopoff, *Science* **236**, 1563 (1987).
  - [83] Y. Ogata, *J. American Stat. Assoc.* **83**, 9 (1988).
  - [84] A. Helmstetter, Y. Y. Kagan, and D. D. Jackson, *Bull. Seismol. Soc. America* **96**, 90 (2006).
  - [85] R. Shcherbakov, G. Yakovlev, D. L. Turcotte, and J. B. Rundle, *Phys. Rev. Lett.* **95**, 218501 (2005).
  - [86] R. Shcherbakov, D. L. Turcotte, and J. B. Rundle, *Bull. Seismol. Soc. America* **96**, 376 (2006).
  - [87] O. Sporns, D. R. Chialvo, M. Kaiser, and C. C. Hilgetag, *Trends in Cognitive Sciences* **8**, 418 (2004).
  - [88] J.-P. Eckmann, S. O. Kamphorst, and D. Ruelle, *Europhys. Lett.* **4**, 973 (1987).